J. CONTAM. HYDROL. 61, 131-145

INFLUENCE OF THE MODE OF MATRIX POROSITY DETERMINATION ON MATRIX DIFFUSION CALCULATIONS

K. Ota [a, *], A. Möri [b], W. R. Alexander [c], B. Frieg [c] and M. Schild [d]
[a] JNC (Japan Nuclear Cycle Development Institute), Tono Geoscience Centre, Toki, Japan
[b] Geotechnical Institute Ltd, Berne, Switzerland
[c] Nagra (National Cooperative for the Disposal of Radioactive Waste), Wettingen, Switzerland
[d] Institut für Geologie und Dynamik der Lithosphäre, University of Göttingen, Germany

Abstract

The theoretical basis for matrix diffusion in fractured rocks and the methodology for the determination of diffusion coefficients in the laboratory are well established. One significant problem, however, remains in that it is difficult to quantify the degree of sample disturbance affecting the geometrical, geophysical and hydraulic properties of the rock matrix.

A new technique, with *in situ* rock impregnation with resin, for examining the diffusion-accessible rock matrix has been developed and successfully adopted to the rock matrix behind a water-conducting fracture in host crystalline rocks at Nagra's Grimsel Test Site in Switzerland and JNC's Kamaishi *In Situ* Test Site in Japan. In line with the results of a large number of natural analogue and laboratory studies, the existence of an *in situ* interconnected pore network was substantiated. Matrix porosities determined on the laboratory samples from both the sites are 1.5 to 3 times higher than *in situ* values, irrespective of the technique applied. On the Grimsel granodiorite matrix, matrix porosity existing *in situ* and artefacts of stress release and physical disturbance, induced by sampling and sample preparation, were clearly distinguished, allowing *in situ* porosity to be quantified.

Laboratory work with conventional techniques tends to overestimate the porosity of the rock matrix, hence leading to an overestimation of *in situ* matrix diffusion. The implications of these differences to a repository performance assessment are assessed with a couple of examples from existing assessments and recommendations for future approaches to the examination of *in situ* matrix porosity are made.

Keywords: *In situ* porosity, Artefacts, Diffusion-accessible matrix, Non-conservatism

1. Introduction

The term matrix diffusion is applied to the process by which solute, flowing in distinct fractures, penetrates the surrounding rock. Diffusion into this rock occurs in a connected system of pores or microfractures, and diffusion through the solid phase is insignificant by comparison (*eg* Valkiainen, 1992). The importance of matrix diffusion in the context of a radioactive waste repository is that it provides a mechanism for greatly enlarging the area of rock surface in contact with advecting radionuclides, from that of the fracture surfaces and their infills, to a much larger portion of the bulk rock (*eg* Neretnieks, 1980; Grisak and

---

[*] Corresponding author. Fax: +81-572-55 0180. E-mail address: kunio@tono.jnc.go.jp

Pickens, 1980; Rasmuson and Neretnieks, 1981).

Although the theoretical basis for matrix diffusion is thus fairly well established, the matrix diffusion concept required experimental verification and work has been carried out on various sedimentary rocks (*eg* Garrels et al., 1949; Klinkenberg, 1951; Mazurek et al., 1996) and crystalline rocks (*eg* Bradbury and Stephen, 1986; Skagius and Neretnieks, 1986; Hellmuth, et al., 1992). One significant problem, however, is that the work is conducted, out of necessity, on samples disturbed by collection and preparation. This leads, for example, to de-stressing of the rock (an inevitable consequence of removal to the laboratory) inducing non-reproducible changes to the geometry of matrix porosity. Other perturbations due to sample cutting or grinding will also change both the pore geometry and sorption properties of the rock, which indicates that the laboratory results must be treated with some caution. In general, all of the changes induced in the samples tend to cause overestimation of the rock diffusivity, leading to an overestimation of matrix diffusion which is, in turn, non-conservative in the safety assessment sense as it leads to an apparently greater degree of radionuclide retardation in the geosphere (McKinley, 1989). A large number of attempts have been made to date to assess matrix diffusion by complex laboratory experiments and field experiments but in only a few cases have the experiments provided relevant information. In fact, a study attempted to quantify the degree of disturbance showed that laboratory-produced data probably overestimate *in situ* diffusion coefficients by a factor of 2 to 5 (Skagius, 1986). These should be treated as minimum values, however, as the study was conceptually simplistic, assuming that re-stressing core samples with simulated overburden pressures would represent undisturbed *in situ* conditions. In only a few studies that attempted to measure directly the actual penetration profiles (*eg* Ittner et al., 1988), it is usually shown that the calculated diffusion coefficients are several orders of magnitude greater than *in situ* values.

Nagra (Swiss National Co-operative for the Disposal of Radioactive Waste) and JNC (Japan Nuclear Cycle Development Institute) have been conducting an *in situ* validation of matrix diffusion in parallel with natural analogue studies, as part of the joint Nagra/JNC Radionuclide Retardation Programme based around two underground rock laboratories (URLs): Nagra's Grimsel Test Site (GTS) in the central Swiss Alps and JNC's Kamaishi *In Situ* Test Site (KTS) in north-east Japan (for more details, see Smith et al., 2001, Ota et al., 2001 and Alexander et al., 2002). In this programme, the focus was on a single water-conducting fracture (or a shear zone) and adjacent rock matrix within the Grimsel granodiorite at the GTS and within the Kurihashi granodiorite at the KTS. Natural analogue studies showed that matrix diffusion occurs in the rock matrix close behind the experimental water-conducting fracture at both URLs (Alexander et al., 1990a, b; Ota et al., 1999) and it was decided that this merited further, detailed study. However, in a break from traditional laboratory-based studies of matrix porosity, a new technique, with *in situ* rock impregnation with resin, for the examination of diffusion-accessible matrix was developed and successfully implemented. Here, artefacts associated with the laboratory measurement of porosity can be evaluated and the effects of these artefacts on calculated radionuclide retardation assessed more thoroughly than has previously been the case.

2. Experimental Methodology

In the Nagra/JNC studies, it was intended to examine the matrix porosity behind the water-conducting fractures under undisturbed, *in situ*, conditions and to allow direct comparison of *in situ* values with the large volume of laboratory experimental data available from numerous other studies at both URLs. This required *in situ* immobilisation of the matrix porosity prior to the excavation of the rock mass for further laboratory examination. Several potential methods were assessed (for details, see Möri et al., 2002) and, subsequently, the following techniques were adopted.

2.1. Rock matrix immobilisation and sample recovery

Several parallel injection boreholes were drilled almost perpendicular to the water-conducting fracture. Intervals within the injection boreholes were isolated with mechanical packer systems in a way that the intervals are at least one metre beyond the tunnel wall (avoiding effects of excavation disturbed zone of the tunnel and de-saturation of the matrix) and that there is a continuous profile through the rock matrix on both sides of the water-conducting fracture for several metres.

A specially formulated, fluoresceine-doped acrylic resin was injected, under a small over-pressure for 6 weeks, into the rock matrix at the GTS whereas a fluoresceine-doped epoxy resin developed for this specific aspect of the study was utilised in a similar way at the KTS. Following polymerisation of the resin[†], the impregnated rock volume was excavated by 200mm-diameter overcoring and then returned to the laboratory (Fig. 1; for details, see Frieg et al., 1998).

Sub-samples for further laboratory examination were obtained by sawing the cores in the laboratory. In the case of the comparison of porosity-determining techniques, identical volume sub-samples were obtained from a core slab (Fig. 2). The natural variation in the porosity distribution from these neighbouring samples is unlikely to be significant in these particular samples due to the uniformity of the mineral distribution, but it is clear that, for highly heterogeneous rocks (*eg* a course-grained gneiss), such a comparison could be problematic.

2.2. Microscopical matrix porosity characterisation

Standard petrological observation by fluorescent microscopy and detailed scanning electron microscope (SEM) examination were executed on the sub-samples of *in situ* impregnated rock recovered from both URLs in order to characterise the geometry, distribution and connectivity of rock matrix porosity.

In addition, a series of successive 2-D images of the resin-filled pore space was obtained, using the SEM, by repeatedly grinding and polishing 10µm off the *in situ* impregnated sample and capturing backscattered electron images. Over 50 2-D images were digitised and processed appropriately through several steps of data treatment and finally a 3-D reconstruction of the *in situ* matrix porosity was created.

2.3. Porosity determination

Three different techniques were applied for quantitative porosimetrical investigation on *in situ* and laboratory impregnated samples along with unimpregnated samples from both URLs, so allowing the evaluation of artefacts associated with sample recovery and treatment.

The procedure for *water saturation gravimetry* follows basically the method proposed by

---

[†] To initiate polymerisation of the acrylic resin, downhole heaters raised the rock temperature to between 40 and 60°C up to 25cm away from the injection borehole.

Franklin et al. (1979). A standard *mercury injection porosimetry* was also applied, with maximum injection pressures of about 230MPa and about 400MPa, for the determination of porosity and pore size distribution. Finally, an additional, innovative, new method was applied: direct quantification of the intrusion volume of resin in the *in situ* impregnated samples (*chemical analysis porosimetry*). Here, the fact that the acrylic and epoxy resins employed *in situ* contain carbon and nitrogen respectively as a major constituent element (whereas the rock matrix is, by contrast, originally poor in both elements) was used as a direct indication of *in situ* porosity impregnated (full details of all three techniques presented in Möri et al., 2002).

2.4. Seismic velocity and hydraulic conductivity measurements

Experimental determinations of compressional wave (P-wave) velocity (Vp) and hydraulic conductivity were further performed on the Grimsel granodiorite samples for the quantitative evaluation of porosity as well as the detailed characterisation of the rock matrix (details in Schild et al., 2001).

P-wave velocities were measured on the spherical sub-samples (Ø50mm) of *in situ* impregnated and unimpregnated materials under both dry and water-saturated conditions at varying confining pressures. The measuring system in which the samples were mounted allows a rotation of 360° on the vertical axes and 75° around the horizontal axes, which enables Vp in any direction to be measured with the same precision. The Vp-patterns analysed at over 130 independent measuring directions on both the *in situ* impregnated and unimpregnated samples were compared.

For hydraulic conductivity determination, a pressure transient method using argon gas as a flow medium was applied, with a confining pressure up to 20MPa. Primarily, permeability was estimated following the method presented by Nover et al. (1995) and the hydraulic conductivity was then calculated based upon the estimates of permeability.

3. Results and Discussion

Four types of matrix porosities were distinguished, under UV illumination, in the *in situ* impregnated rock matrix from both URLs (Fig. 3). In order of decreasing abundance, the *in situ* matrix porosity is dominated by enhanced pore spaces that occur along grain boundaries, mostly between quartz, plagioclase and K-feldspar (*grain boundary porosity*). *Sheet silicate porosities* across the cleavage of muscovite, biotite and chlorite are abundant in the vicinity of the water-conducting fracture, where microstructural alteration occurred. Additional pore spaces are provided by *solution porosity* along with exsolution lamellae and twinning within feldspars and by *microfractures* in large grains. Although the precise abundance and distribution of the matrix porosity was strongly affected by the mineralogical and structural heterogeneity of the rock (Möri et al., 2002), these four porosity types, exhibiting an interconnected network, were certainly found throughout the rock matrix at all distances from the water-conducting fracture. Natural analogue studies using disequilibria in the natural decay series demonstrated that matrix diffusion has been occurring in the rock matrix in the immediate vicinity of the water-conducting fractures at the GTS and the KTS (Alexander et al., 1990a, b and Ota et al., 1999 respectively). Taken together, these two independent lines of evidence clearly substantiate the existence of an interconnected matrix porosity that is readily accessible to potential contaminants transported in the water-conducting fractures at these sites.

The architecture of the *in situ* impregnated matrix porosity was found to be similar, but not identical, to that observed in the laboratory impregnated rock matrix. On a micrometre to nanometre scale, detailed SEM examinations revealed the presence of ‘barriers’ that limit resin impregnation (and potentially, therefore, contaminant transport). A microfracture, for instance, is irregularly deformed and often locally kinked to form sharp, angular ‘hinges’. Three-dimensional reconstructions of the *in situ* matrix porosity (Fig. 4) showed higher constrictivity at the hinge and in its immediate vicinity and higher tortuosity along open channels. This suggests that these effects could reduce accessibility of diffusing contaminants *in situ* to the rock matrix despite the existence of an interconnected network. More importantly, the absence of such constrictions in the laboratory samples will clearly produce unrealistically high estimates of matrix accessibility and associated diffusion coefficient measurements, providing non-conservative estimates of rock matrix contaminant retardation capacity.

A comparison of the results of laboratory porosity determinations using three different techniques shows a generally good agreement (Table 1). Within the sampling limitations noted above, the agreement provides a convincing demonstration of the consistency of these techniques. The laboratory-impregnated and unimpregnated samples have porosities of 0.53–0.80vol% for the Grimsel granodiorite matrix, irrespective of the techniques applied, and 3.81–4.01vol% and 2.20–2.27vol% for the hydrothermally altered and weakly altered matrices respectively of the Kurihashi granodiorite. These values are consistent with laboratory porosimetry data previously reported for both the Grimsel granodiorite (*eg* Meyer et al., 1989; Bossart and Mazurek, 1991) and the Kurihashi granodiorite (Sato et al., 1997).

In situ porosities determined by chemical analysis porosimetry have average values of 0.27vol% for the Grimsel granodiorite matrix and of 2.76vol% and 1.18vol% for the hydrothermally altered and weakly altered Kurihashi granodiorite matrices respectively (Table 1). These values are 1.5 to 3 times lower than those measured on the laboratory samples. In addition, the *in situ* impregnated samples were further impregnated with mercury in the laboratory, producing ‘additional’ porosity values of 0.39–0.41vol% (for the Grimsel granodiorite matrix). This is consistent with the differences (0.26–0.53vol%) between the *in situ* and laboratory determined porosity values (Table 1). Combined with the observations, described above, on the differences in pore geometry between both sample sets, this strongly suggests that the higher porosity values observed in the laboratory samples are due to the opening up of the hinge-type barriers present in the *in situ* matrix porosity and the creation of new types of pores. Geometrical changes to the existing matrix porosity are most likely induced by stress release after core recovery and physical disturbance during sample treatment in the laboratory. This is supported by pore size distribution data: the relative abundance of the artificial pores with equivalent diameters below a few micrometres is much lower than that of laboratory-observed (*ie in situ* plus artificial) pores whereas the relative abundance curves for both pore types, over a few micrometres in size, are consistent (Fig. 5). Here, the consistency is an obvious indication of that larger pores with equivalent diameters over a few micrometres are not present *in situ*.

Similar results were demonstrated for the P-wave velocity and the hydraulic conductivity of the Grimsel granodiorite matrix. The Vp values for the *in situ* impregnated samples are higher under water-saturated conditions than those under dry conditions (Fig. 6). This is due to the limited compressibility of water-saturated pores compared with that of air-filled pores and indicates that the *in situ* impregnated samples have additional (*ie* artificial) pores. Since the ΔVp patterns for the *in situ* impregnated and unimpregnated samples reflect the influence of the saturation of artificial and *in situ* plus artificial pores respectively, the degree of influence of *in situ* matrix porosity can be expressed as the discrepancy of both the ΔVp patterns (Fig. 6). The ΔVp pattern for the *in situ* matrix pores agrees with that obtained for the artificial pores. This suggests that about 50% of the laboratory-observed porosity is the artificial pores, which is in agreement with the porosimetrical investigations, discussed above. In addition, a ΔVp stereogram for the matrix porosity impregnated *in situ* indicates that grain boundary and sheet silicate porosities significantly contributed to the *in situ* matrix porosity (Schild et al., 2001). It is obvious that these matrix porosities control the directional dependence of the hydraulic properties of the Grimsel granodiorite matrix. The hydraulic conductivity is higher parallel to the rock foliation and, in general, the unimpregnated samples yielded hydraulic conductivity values about 1.5 to 7.5 times higher than the *in situ* impregnated samples (Table 2), which indicates that the influence of sampling and handling artefacts on hydraulic properties is significant. Similar results were obtained in the Lac du Bonnet granite with laboratory permeabilities 2 to 3 orders of magnitude greater than *in situ* values (Vilks et al., 1999).

A direct comparison of porosity values determined on the laboratory samples with the *in situ* values derived in these studies clearly demonstrated that 30 to 60% of the porosity measured by conventional laboratory techniques is artefacts of stress release and physical disturbance. The adoption of the laboratory definition of porosity directly to *in situ* conditions will lead to the effect of increasing the values of measured diffusion coefficients, underestimating the role of size and charge exclusion effects in the rock matrix and, consequently, overestimating matrix diffusion *in situ*. Möri et al. (2002) re-ran some transport calculations for ^{79}Se, ^{135}Cs, ^{99}Tc and ^{237}Np using a data set modified from Nagra’s Kristallin-I and JNC’s H12 performance assessments (Nagra, 1994 and JNC, 2000 respectively) in order to assess the significance of the differences observed on calculated radionuclide releases. Of all the realisations run, it is clear that the depth of diffusion-accessible matrix is a more important parameter than the matrix porosity and the matrix pore diffusion coefficient. Assuming a reduced matrix depth gives rise to both earlier and higher geosphere releases whereas an increased depth, while producing little temporal change in the release pattern, significantly decreases the peak release concentration.

It should be noted again that an interconnected pore network spreads throughout the rock matrix on both sides of the water-conducting fracture for, at least, several metres at both URLs. Indeed, once outside the zone of influence of the water-conducting fracture (a few decimetres deep at most), there is little obvious difference in the geometry of matrix porosity and it is therefore tempting to suggest that the entire rock matrix is, in principle, open to diffusive transport of contaminants. This is certainly in agreement with natural analogue evidence from other crystalline and sedimentary rocks (*eg* Alexander et al., 1990a; Hofmann, 1990), which indicates that connected porosity can extend for decametres in some cases. It is therefore strongly recommended that further studies on *in situ* matrix porosity be executed and it is clear that these studies should focus on defining the depth of matrix connectivity in a range of rock types in order to validate existing data sets.

4. Conclusions

In line with a large number of natural analogue and laboratory studies, there is certainly evidence that *in situ* diffusion-accessible porosity exists in the rock matrix in different host crystalline rocks and forms an interconnected network (of four types of porosities) that extends to considerable depths in the rocks. In addition, artefacts of stress release and physical disturbance, which are inevitable in recovering cores and treating samples in the laboratory, have been well defined and clearly shown to induce non-reproducible changes to the geometry and connectivity of *in situ* matrix porosity (and specifically, the complex effects of the alteration of the existing matrix porosity and the creation of new types of pores), enhancing the matrix porosity by a factor of 1.5 to 3. However, the degree of non-conservatism led by the adoption of laboratory-derived data appears to be low on calculated radionuclide retardation in the geosphere. Rather, the depth of diffusion-accessible matrix behind water-conducting fractures is of much more significance in a repository performance assessment. It is therefore necessary to make further assessments on the extent of *in situ* matrix connectivity in a range of rock types (and eventually, in repository host rocks) for the future repository performance assessment.

Finally, the present study has demonstrated that the combination of novel *in situ* rock impregnation methods and innovative laboratory techniques, which were developed at both URLs, has indeed proven to be effective for the examination of diffusion-accessible matrix and the quantitative evaluation of *in situ* porosity. This represents another important step towards more realistic representation of *in situ* rock matrix properties, which are of significance in the assessment of likely radionuclide retardation in fractured rocks.

Acknowledgements

Many colleagues in both Switzerland and Japan contributed to the work described here but we would particularly like to thank M. Mazurek (University of Berne), C. Bühler (Solexperts, Zürich), H. Dollinger (Geotechnical Institute, Solothurn), P. Haag (Sika, Zürich) and T. Ando (JNC Tono Geoscience Centre). Finally, the authors would like to thank both Nagra and JNC for funding this work under the auspices of the joint Nagra/JNC Radionuclide Retardation Programme.

References

Alexander, W.R., MacKenzie, A.B., Scott, R.D., McKinley, I.G., 1990a. Natural analogue studies in crystalline rock: the influence of water-bearing fractures on radionuclide immobilisation in a crystalline rock repository. Nagra Technical Report NTB 87-08, Nagra, Wettingen, Switzerland.

Alexander, W.R., McKinley, I.G., MacKenzie, A.B., Scott, R.D., 1990b. Verification of matrix diffusion by means of natural decay series disequilibria in a profile across a water conducting fracture in granitic rock. Sci. Basis Nucl. Waste Manag. XIII, 567–576.

Alexander, W.R., Ota, K., Möri, A., 2002. An overview of the results of the 15 year long Nagra-JNC Radionuclide Migration Programme. Geochem. Trans. (in preparation)

Bradbury, M.H., Stephen, I.G., 1986. Diffusion and permeability based sorption measurements in intact rock samples. Sci. Basis Nucl. Waste Manag. IX, 81–90.

Bossart, P., Mazurek, M., 1991. Structural geology and water flow-paths in the migration shear zone. Nagra Technical Report NTB 91-12, Nagra, Wettingen, Switzerland.

Franklin, J.A.M., Vogler, U.W., Szlavin, J., Edmond, J.M., Bieniawski, Z.T., 1979. Suggested methods for determining water content, porosity, density, adsorption and related properties and swelling and slake-durability index properties. In: Brown, E.T. (Ed), Rock

Characterization Testing and Monitoring, ISRM Suggested Methods. Pergamon Press, Oxford, pp. 81–94.

Frieg, B., Alexander, W.R., Dollinger, H., Bühler, C., Haag, P., Möri, A., Ota, K., 1998. In situ resin impregnation for investigating radionuclide retardation in fractured repository host rocks. J. Contam. Hydrol. 35, 115–130.

Garrels, R.M., Dreyer, R.M., Howland, A.L., 1949. Diffusion of ions through intergranular spaces in water saturated rocks. Bull. Geol. Soc. Amer. 60, 1809–1924.

Grisak, G.E., Pickens, J.F., 1980. Solute transport through fractured media, part I: the effect of matrix diffusion. Water Resour. Res. 16, 719–730.

Hellmuth, K.-H., Siitari-Kauppi, M., Lindberg, A., 1992. Applications of the carbon-14-polymethacrylate (PMMA) impregnation method in studies on porosity and matrix diffusion. Sci. Basis Nucl. Waste Manag. XV, 649–656.

Hofmann, B.A., 1990. Reduction spheroids from northern Switzerland: mineralogy, geochemistry and genetic models. Chem. Geol. 81, 55–81.

Ittner, T., Trostenfelt, B., Allard, B., 1988. Diffusion of Np, Pu and Am in granitic rock. Radiochim. Acta 44/45, 171–177.

JNC, 2000. H12: Project to establish the scientific and technical basis for HLW disposal in Japan. JNC Technical Reports JNC TN1410 2000-001–005, JNC, Tokai, Japan.

Klinkenberg, L.J., 1951. Analogy between diffusion and electrical conductivity in porous rocks. Bull. Geol. Soc. Amer. 62, 559–568.

Meyer, J., Mazurek, M., Alexander, W.R., 1989. Petrographic and mineralogical characterisation of fault zones AU96 and AU126. In: Bradbury, M.H. (Ed), Grimsel Test Site - Laboratory Investigations in Support of the Migration Experiments, Chapter 2. Nagra Technical Report NTB 88-23, Nagra, Wettingen, Switzerland.

Mazurek, M., Alexander, W.R., MacKenzie, A.B., 1996. Contaminant retardation in fractured shales: matrix diffusion and redox front entrapment. J. Contam. Hydrol. 21, 71–84.

McKinley, I.G., 1989. Applying natural analogues in predictive performance assessment. Nagra Internal Report, Nagra, Wettingen, Switzerland.

Möri, A., Schild, M., Siegesmund, S., Vollbrecht, A., Adler, M., Mazurek, M., Ota, K., Haag, P., Ando, T., Alexander, W.R., 2002. The Nagra-JNC in situ study of safety relevant radionuclide retardation in fractured crystalline rock IV: the in situ study of matrix porosity in the vicinity of a water-conducting fracture. Nagra Technical Report NTB 00-08, Nagra, Wettingen, Switzerland.

Nagra, 1994. Kristallin-1: Safety assessment report. Nagra Technical Report NTB 93-22, Nagra, Wettingen, Switzerland.

Neretnieks, I., 1980. Diffusion in the rock matrix: an important factor in radionuclide retardation? J. Geophys. Res. 85, 4379–4397.

Nover, G., Heikamp, S., Kotny, A., Duba, A., 1995. The effect of pressure on the electrical conductivity of KTB rocks. Surv. Geophys. 16, 63–81.

Ota, K., Amano, K., Ando, T., 1999. Brief overview of in situ nuclide retardation in a fractured crystalline rock, Kamaishi In Situ Test Site. In: Proceedings of an International Workshop for the Kamaishi In Situ Experiments, Kamaishi, Japan, 24-25 August 1998. JNC Technical Report JNC TN7400 99-007, JNC, Toki, Japan, pp. 67–76.

Ota, K., Alexander, W.R., Smith, P.A., Möri, A., Frieg, B., Frick, U., Umeki, H., Amano, K., Cowper, M.M., Berry, J.A., 2001. Building confidence in radionuclide transport models for fractured rock: the Nagra/JNC Radionuclide Retardation Programme. Sci. Basis Nucl. Waste Manag. XXIV, 1033–1041.

Rasmuson, A., Neretnieks, I., 1981. Migration of radionuclides in fissured rock: the influence of micropore diffusion and longitudinal dispersion. J. Geophys. Res. 86, 3749–3578.

Sato, H., Shibutani, T., Tachi, Y., Ota, K., Amano, K., Yui, M., 1997. Diffusion behaviour of nuclide pathways in fractured crystalline rocks. JNC Technical Report PNC TN8410 97-127, JNC, Tokai, Japan.

Schild, M., Siegesmund, S., Vollbrecht, A., Mazurek, M., 2001. Characterization of granite matrix porosity and pore-space geometry by in situ and laboratory methods. Geophys. J. Int. 146, 111–125.

Skagius, K., 1986. Diffusion of dissolved species in the matrix of some Swedish crystalline rocks. PhD Thesis, Royal Institute of Technology, Stockholm, Sweden.

Skagius,K., Neretnieks, I., 1986. Porosities and diffusivities of some nonsorbing species in crystalline rocks. Water Resour. Res. 22, 389–397.

Smith, P.A., Alexander, W.R., Kickmaier, W., Ota, K., Frieg, B., McKinley, I.G., 2001. Development and testing of radionuclide transport models for fractured rock: examples from the Nagra/JNC Radionuclide Migration Programme in the Grimsel Test Site, Switzerland. J. Contam. Hydrol. 47, 335–348.

Valkiainen, M., 1992. Diffusion in the rock matrix – a review of laboratory tests and field studies. Report YJT-92-04, Nuclear Waste Commission of Finnish Power Companies, Helsinki, Finland.

Vilks, P., Cramer, J.J., Melnyk, T.W., Stanchell, F.W., Miller, N.H., Miller, H.G., 1999. In-situ diffusion in granite: phase I final report. Report No. 06819-REP-01200-0087-R00, Ontario Power Generation, Nuclear Waste Management, Toronto, Canada.

Fig. 1: Methodology of *in situ* resin impregnation at the GTS; (A) injection of the acrylic resin into the rock matrix, (B) polymerisation of the resin by heating, (C) large-diameter overcoring of the resin impregnated rock volume and (D) sub-sampling and sample preparation for further laboratory examination. Same experimental procedure except for the step B (heating) applied at the KTS.

Fig. 2: Sub-sampling from the *in situ* resin impregnated core slab for quantitative porosimetrical investigations.

Fig. 3: Architecture of *in situ* matrix porosity; (a) grain boundary porosity in quartz ribbons, (b) sheet silicate porosity in a mica band, (c) solution porosity in sericitised parts in a large plagioclase grain and (d) microfractures in a large K-feldspar grain with perthitic exsolution lamellae. Photomicrographs taken under crossed polars (left) and under UV illumination (right).

Fig. 4: 3-D reconstructions, from different viewpoints, of the *in situ* porosity existing in the Grimsel granodiorite matrix, showing the ‘channel and barrier’ structure. Sample size (length x width x thickness): 4.13 x 1.69 x 0.50mm.

Fig. 5: Size distribution of mercury-injectable porosity in the Grimsel granodiorite matrix. The unimpregnated (C and D) and *in situ* impregnated (E and F) samples showing the relative abundance of laboratory-observed (*ie in situ* plus artificial) and artificial pore size distributions respectively.

Fig. 6: Seismic velocity (Vp) patterns for the *in situ* impregnated and unimpregnated Grimsel granodiorite samples under both water-saturated and dry conditions. A ΔVp stereogram is given by the difference between Vp values under water-saturated and dry conditions. Schmidt net, lower hemisphere. Vp unit: kms^{-1}.

Table 1: Porosities of the Grimsel granodiorite matrix and the different rock matrices of the Kurihashi granodiorite, determined by three different techniques.

Table 2: Hydraulic conductivities of the *in situ* impregnated and unimpregnated rock matrices of the Grimsel granodiorite at confining pressures of 5 and 20MPa.

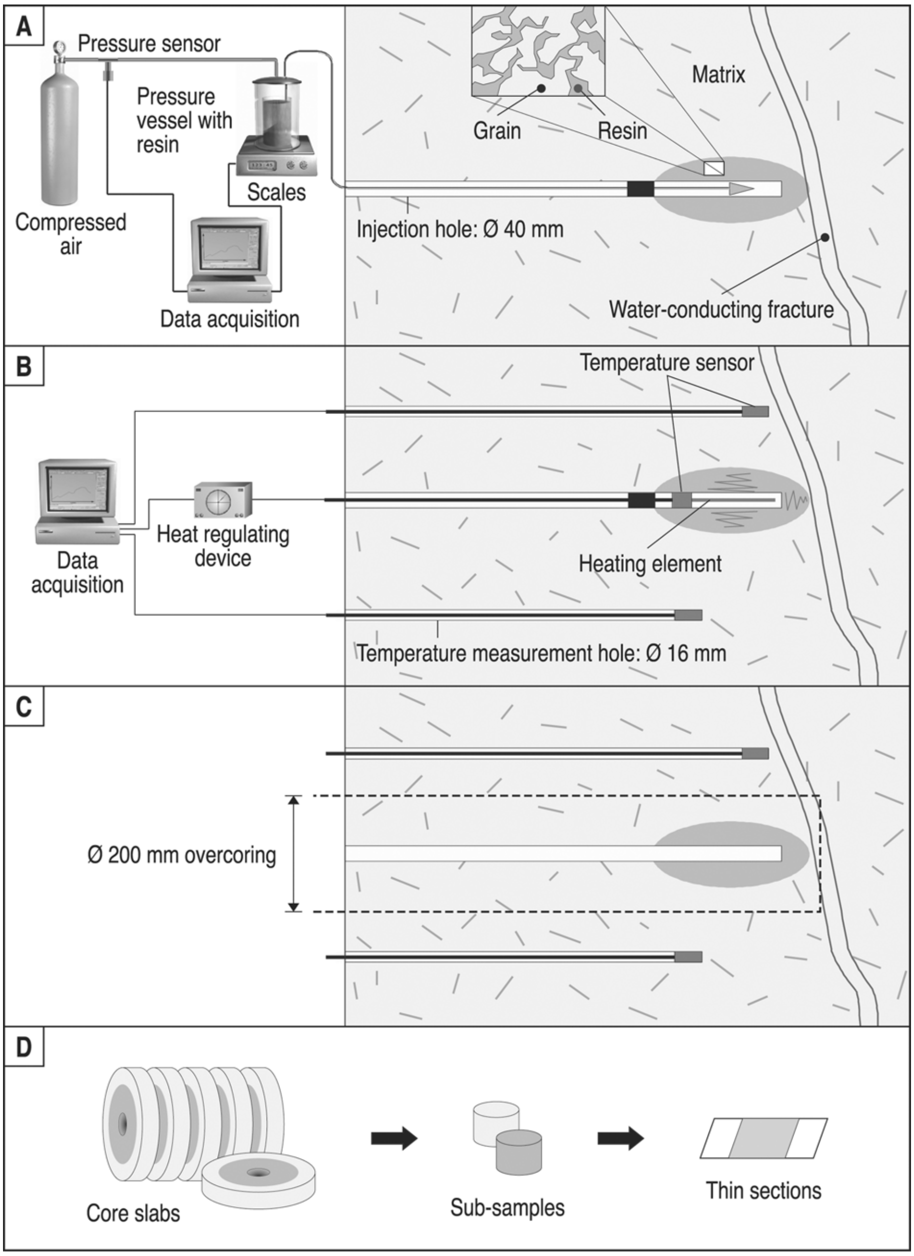
A
Pressure sensor
Pressure vessel with resin
Scales
Compressed air
Data acquisition
Matrix
Grain
Resin
Injection hole: Ø 40 mm
Water-conducting fracture
B
Temperature sensor
Data acquisition
Heat regulating device
Heating element
Temperature measurement hole: Ø 16 mm
C
Ø 200 mm overcoring
D
Core slabs
Sub-samples
Thin sections

Fig. 1

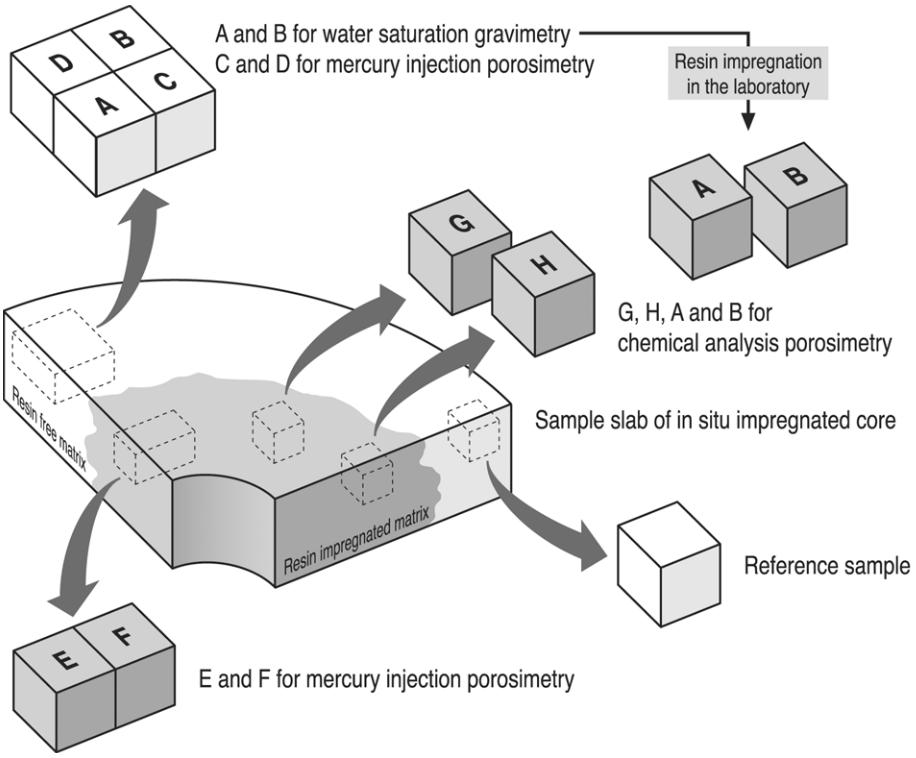
D
B
A
C
A and B for water saturation gravimetry
C and D for mercury injection porosimetry
Resin impregnation
in the laboratory
A
B
G
H
G, H, A and B for
chemical analysis porosimetry
Resin free matrix
Sample slab of in situ impregnated core
Resin impregnated matrix
Reference sample
E
F
E and F for mercury injection porosimetry

Fig. 2

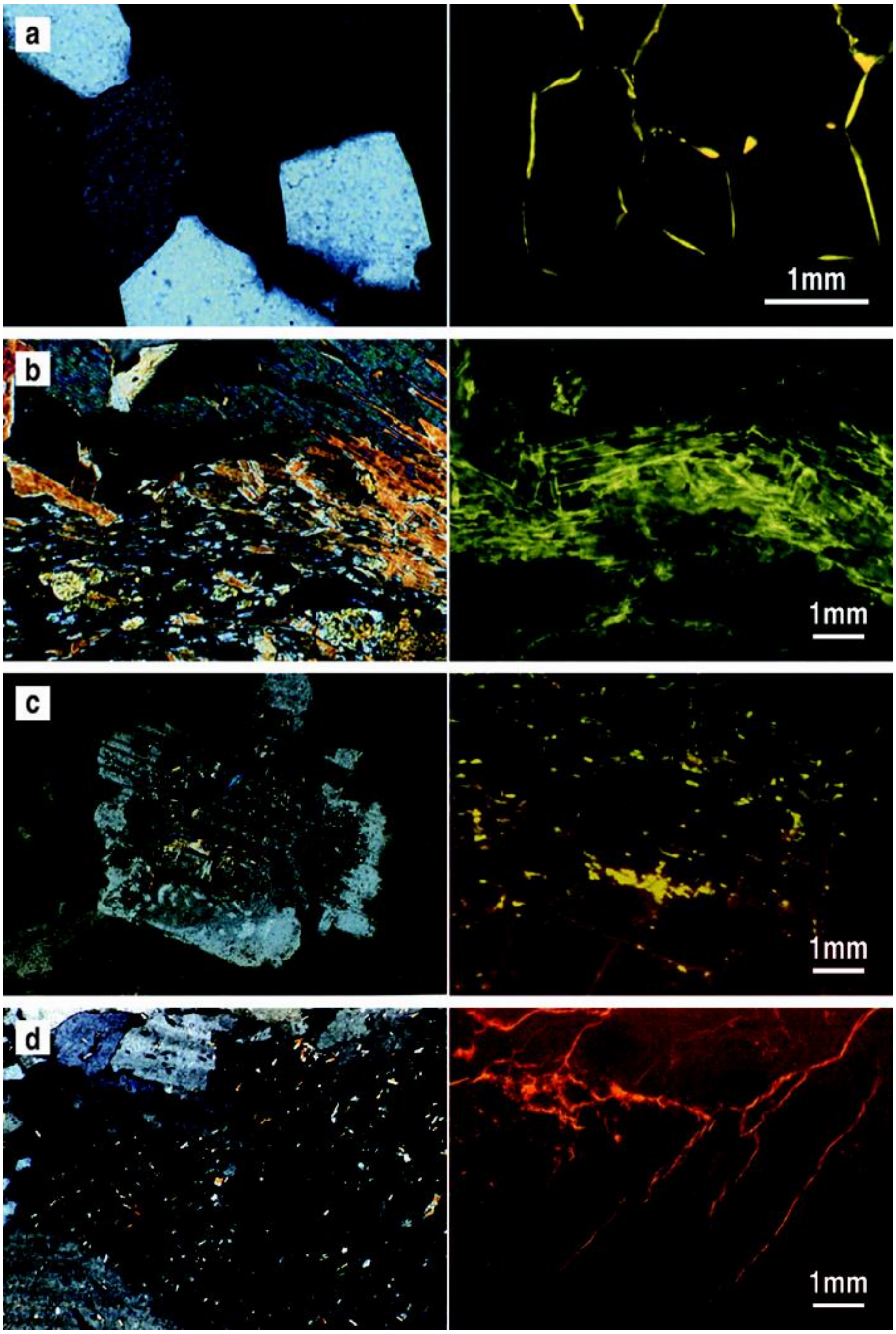

Fig. 3

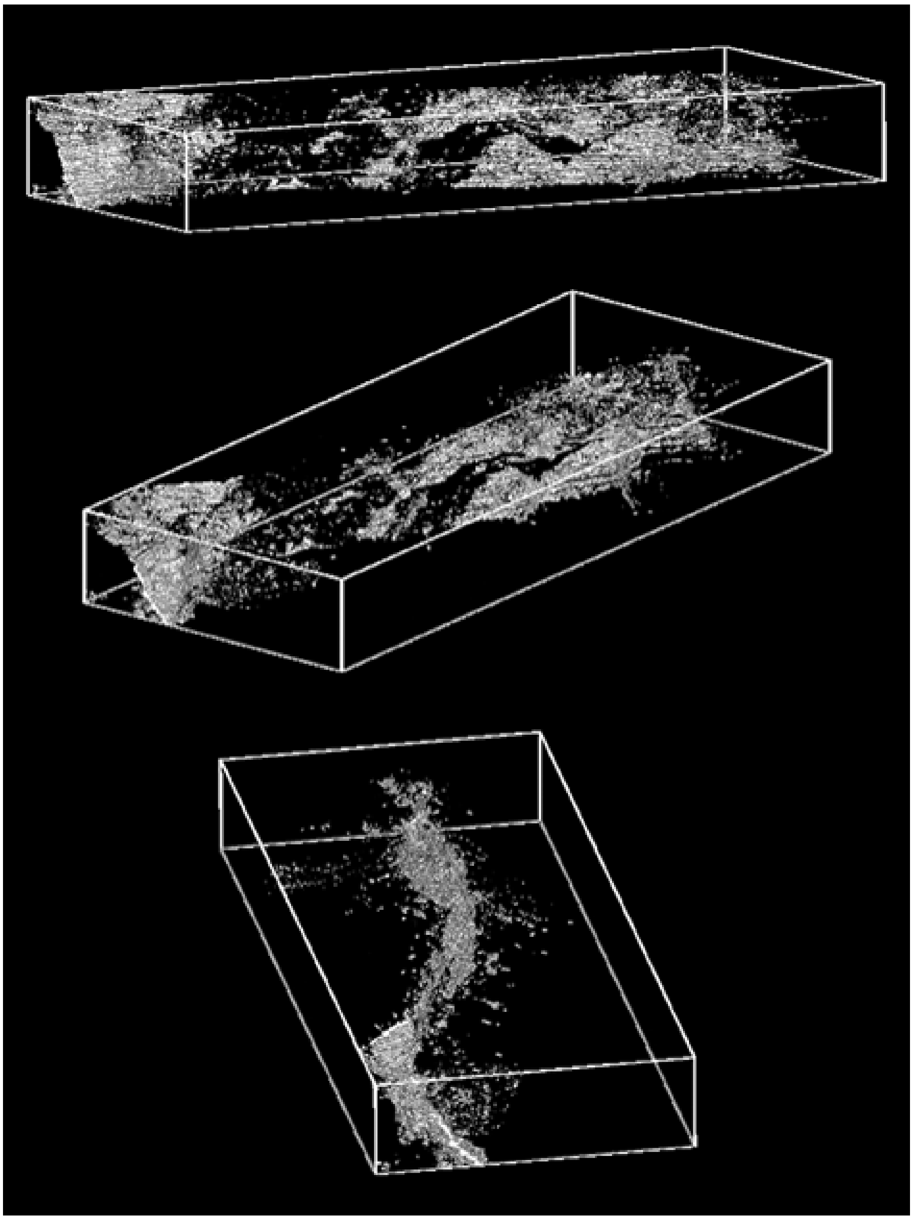

Fig. 4

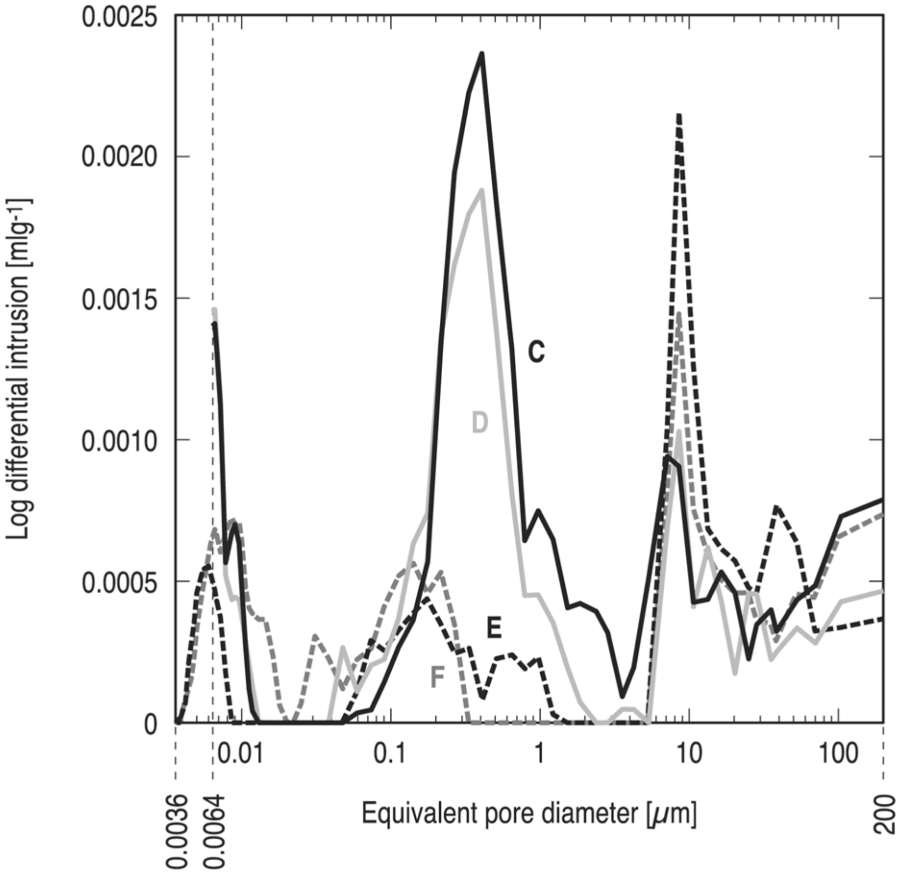
0.0025
0.0020
0.0015
0.0010
0.0005
0
Log differential intrusion [mlg-1]
C
D
E
F
0.01
0.1
1
10
100
0.0036
0.0064
200
Equivalent pore diameter [μm]

Fig. 5

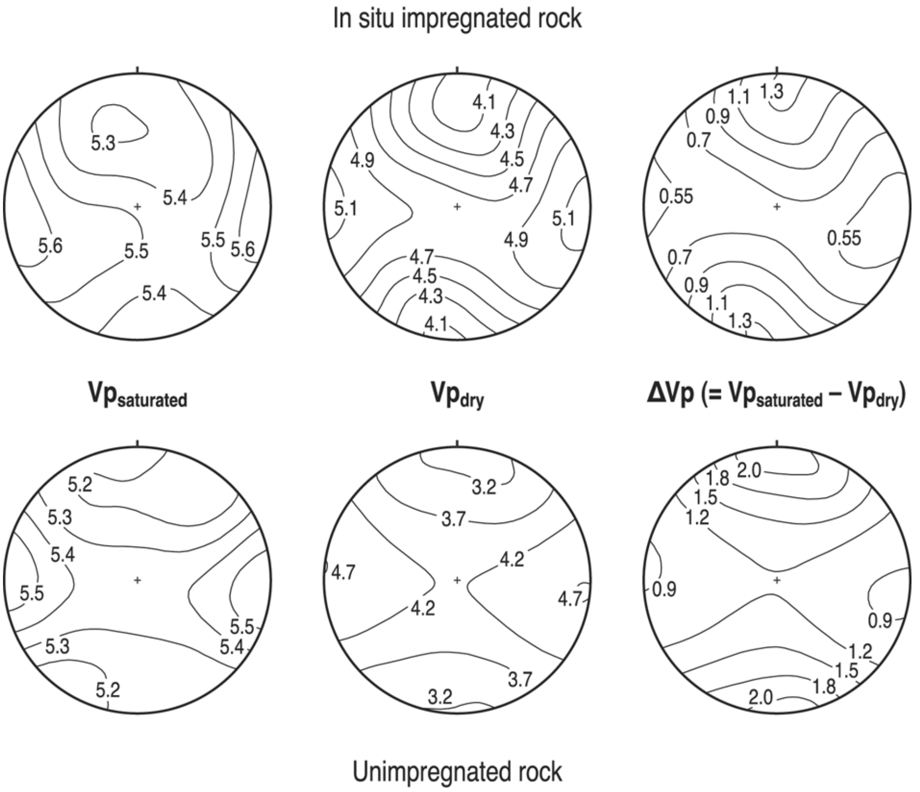
In situ impregnated rock
5.3
5.4
5.6
5.5
5.5
5.6
5.4
4.1
4.3
4.5
4.7
4.9
5.1
5.1
4.9
4.7
4.5
4.3
4.1
1.1
1.3
0.9
0.7
0.55
0.55
0.7
0.9
1.1
1.3
Vp$_{saturated}$
Vp$_{dry}$
ΔVp (= Vp$_{saturated}$ – Vp$_{dry}$)
5.2
5.3
5.4
5.5
5.5
5.4
5.3
5.2
3.2
3.7
4.2
4.7
4.2
4.7
3.7
3.2
1.8
2.0
1.5
1.2
0.9
0.9
1.2
1.5
1.8
2.0
Unimpregnated rock

Fig. 6

Table 1

Techniques and samples	Matrix porosity determined	Porosity values [vol %]		
		GTS: unaltered matrix	KTS: Hydrothermally altered matrix	KTS: Weakly altered matrix
Water saturation gravimetry				
• unimpregnated sample	*in situ* + artificial	0.66±0.08 (A) [a]	nd [b]	2.20±0.20
		0.77±0.17 (B)		
Mercury injection porosimetry				
• unimpregnated sample	*in situ* + artificial	0.69±0.01 (C)	3.81±0.08	2.27±0.05
		0.53±0.01 (D)	4.01±0.08	2.24±0.04
• *in situ* impregnated sample	artificial	0.39±0.01 (E)	nd	nd
		0.41±0.01 (F)		
Chemical analysis porosimetry				
• lab-impregnated sample	*in situ* + artificial	0.68±0.01 (A)	nd	2.26±0.02
		0.80±0.01 (B)		
• *in situ* impregnated sample	*in situ*	0.21±0.02 (G)	2.69±0.11	1.03±0.12
		0.33±0.01 (H)	2.82±0.04	1.33±0.04

[a] Sub-sample number in parenthesis corresponding to that given in Figure 2.
[b] Not determined.

Table 2

Samples	Hydraulic conductivity [ms^{-1}]		
	Direction [a]	5MPa [b]	20MPa [b]
***In situ* impregnated sample**	x	7.89×10^{-12}	2.89×10^{-12}
	z	8.93×10^{-13}	2.67×10^{-13}
Unimpregnated sample	x	1.90×10^{-11}	4.89×10^{-12}
	z	6.72×10^{-12}	1.69×10^{-12}

[a] Measurement direction parallel (x) and perpendicular (z) to the rock structure.
[b] Confining pressure.